NUMERICAL STUDY OF DAMAGES IN BRIDGE SURFACING STRUCTURES BY FIVE-POINT BENDING TESTS

J. Li[1], X. Liu[2], C. Kasbergen[3], G. Tzimiris[4], A. Scarpas[5]

(1) Corresponding author
Section of Road and Railway Engineering, Delft University of Technology
Stevinweg 1, 2628 CN Delft, the Netherlands
Phone: + 31 (0)15 27 84676
Email: jinlong.li@tudelft.nl

(2) Section of Road and Railway Engineering, Delft University of Technology
Stevinweg 1, 2628 CN Delft, the Netherlands
Phone: + 31 (0)15 27 87918
Email: x.liu@tudelft.nl

(3) Section of Road and Railway Engineering, Delft University of Technology
Stevinweg 1, 2628 CN Delft, the Netherlands
Phone: + 31 (0)15 27 82729
Email: c.kasbergen @tudelft.nl

(4) Section of Road and Railway Engineering, Delft University of Technology
Stevinweg 1, 2628 CN Delft, the Netherlands
Phone: + 31 (0)15 27 89388
Email: g.tzimiris@tudelft.nl

(5) Section of Road and Railway Engineering, Delft University of Technology
Stevinweg 1, 2628 CN Delft, the Netherlands
Phone: + 31 (0)15 27 84017
Email: a.scarpas@tudelft.nl

Submission Date: 30/07/2013
Word Count:

Body Text = 3020

Abstract = 125

Figures 11×250 = 2750

Tables 2×250 = 500

Total = 6395

ABSTRACT

Orthotropic steel deck bridges (OSDBs) are widely used in long-span or movable bridges around the world. In the Netherlands, the surfacing structure of OSDBs mostly consists of multiple material layers. Early or accumulated damages of multilayer surfacing systems is a complicated and yet not properly solved technical problem. A three dimensional elasto-visco-plastic model based on the generalized Burger's model was developed and implemented in CAPA-3D for simulating fatigue damages in asphaltic materials. The material model was calibrated and verified by five-point bending fatigue tests on beam specimens of multilayer bridge surfacing structures. The FE model is capable of simulating accumulations and distributions of damages in asphalt surfacing structures, and could be utilized as an auxiliary method to evaluate and design surfacing systems for OSDBs.

Keywords: damage; orthotropic steel deck bridge; fatigue; FEM

INTRODUCTION

Since the first orthotropic steel deck bridge (OSDB) was opened in 1950 over the Neckar River in Mannheim, Germany, the OSDB has become a popular economical alternative when the following issues are important: lower mass, ductility, thinner or shallower sections, rapid bridge installation, and cold-weather construction (*1*). Nowadays more than 1000 orthotropic steel bridges have been built in Europe, out of which 86 are in the Netherlands. OSDBs are also popular in Asia and especially in China and Japan. The application of OSDBs is developing fast in China (*2*).

In the Netherlands, an asphaltic surfacing structure for orthotropic steel bridge decks mostly consists of two structural layers. The upper layer consists of porous asphalt (PA) because of reasons related to noise reduction. For the lower layer a choice between mastic asphalt (MA), or guss asphalt (GA), can be made. Mostly, various membrane layers are involved, functioning as bonding layer, isolation layer as well as adhesion layer.

The asphalt surfacing structures for OSDBs is a complicated and yet not properly solved technical problem. The high flexibility and large local deformations, wind and earthquake forces, temperatures and other natural factors make the problem even more complicated. Due to the special characteristics of OSDBs, fatigue cracking, rutting, delaminating and other damage types are commonly reported and these severely destroy the performance of steel bridges. fatigue damage can also occur at the interface regions between the membrane layers and the surfacing layers but, also, within the membrane materials. It is necessary to study into the damage mechanism, distributions, evolution etc. in the surfacing systems on OSDBs. Laboratory or in-site field tests of damages on bridge pavements are quite costly in time as well as the budget. Proper FE models are always helpful and economical as an auxiliary method.

A material subjected to cyclic loading will accumulate damage and it will fail when the accumulated damage exceeds a threshold. Miner (*3*) was one of the first to relate failure of a material to damage. Since then, a multitude of methods have been developed for quantification of damage. For an excellent review of methods and techniques related to damage prediction in asphalt concrete pavements the reader is referred to Kim and Little (*4*) and Lee and Kim (*5*).

In this paper, firstly, a three dimensional Elasto-Visco-Plastic (EVP) model based on the generalized Burger's model is presented for the simulation of fatigue damages in asphalt materials. The numerical algorithms for the proposed model were implemented in finite element code CAPA-3D (*6*). Secondly, the model was calibrated and verified by comparing the model predictions and experimental tests on 5-points bending(5PB) test specimens (*7*). By using the proposed model, the development of fatigue damage and the severe damage locations in 5PB beam are investigated. Thirdly, the evolution of damages for four selected multilayer surfacing systems on an at temperatures $+10^{o}$C are simulated. Finally, conclusions and suggestions are presented.

This paper has already been published at TRB 2014, however for local dissemination purposes the paper is incorporated within the publications of the Infradagen 2014.

CONSTITUTIVE MODEL

The mechanical analog of a three dimensional Elasto-Visco-Plastic (EVP) model is shown in Figure 1. The model comprises of a linear elastic, a viscoplastic and a number of viscoelastic elements. The strains for each component are additive while all components are subjected to the same stress (i.e. series model).

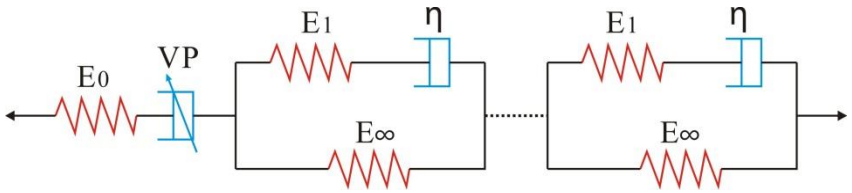

FIGURE 1 Mechanical analog of Elasto-Visco-Plastic (EVP) Model

In incremental formulation it holds:

$$\Delta\boldsymbol{\varepsilon}_{t+\Delta t} = \Delta\boldsymbol{\varepsilon}^{el}_{t+\Delta t} + \Delta\boldsymbol{\varepsilon}^{ve}_{t+\Delta t} + \Delta\boldsymbol{\varepsilon}^{vp}_{t+\Delta t} \tag{1}$$

$$\boldsymbol{\sigma}_{t+\Delta t} = \mathbf{D}^{e} : \boldsymbol{\varepsilon}^{el}_{t+\Delta t} \tag{2}$$

$$F\left(\boldsymbol{\sigma}_{t+\Delta t}, \alpha_{t+\Delta t}\right) = 0 \tag{3}$$

$$\Delta\boldsymbol{\varepsilon}^{vp}_{t+\Delta t} = \Gamma \cdot \langle \Phi \rangle \frac{\partial Q/\partial\sigma}{\left\|\partial Q/\partial\sigma\right\|}\Delta t \tag{4}$$

$$\Delta\alpha = \Gamma \cdot \langle \Phi \rangle \cdot g\left(\boldsymbol{\sigma}_{t+\Delta t}, \alpha_{t+\Delta t}\right)\Delta t \tag{5}$$

where $\Delta\varepsilon$, $\Delta\varepsilon^{el}$, $\Delta\varepsilon^{ve}$, $\Delta\varepsilon^{vp}$ are the total, elastic, viscoelastic and viscoplastic strain components and t is time. $\mathbf{D}^{e}$ in Eq.(2) is the elastic constitutive tensor.

Eq. (3) is the yield function and Eq.(5) describes the evolution of the hardening/softening parameters. The chosen form of the yield function will be presented in the next section.

Eq. (4) is the Perzyna model that define the visoplastic strain incremental tensor $\Delta\boldsymbol{\varepsilon}^{vp}_{t+\Delta t}$. Q is the plastic potential function. Q=F for associated plasticity. Φ is the flow function, which is expressed in terms of F as :.

$$\left\langle \Phi\left(\frac{F}{F_0}\right)\right\rangle = \begin{cases} \Phi\left(\dfrac{F}{F_0}\right) & \text{if } \dfrac{F}{F_0} > 0 \\ 0 & \text{if } \dfrac{F}{F_0} \le 0 \end{cases} \tag{6}$$

The angle bracket < > implies the McCauley switch-on-switch-off operator , F_0 is a reference value of F or any appropriate constant (e.g., yield stress σ_y, atmospheric pressure constant p_a) so as to render F/F_0 dimensionless. The flow function Φ in this thesis is expressed in the term of F as:

$$\Phi = \left(\frac{F}{p_a}\right)^{N} \tag{7}$$

where N is the viscosity index that controls the rate of Φ.

Parameter Γ in Eq. (4) is postulated to be a function of the viscoplastic deformation history. In the framework of this investigation, on the basis of laboratory tests for the mixture, the following relationship is proposed between Γ and the equivalent viscoplastic strain ξ:

$$\Gamma = \Gamma_{min} + \left(\Gamma_{max} - \Gamma_{min}\right)\cdot e^{-k_1\cdot\xi} \tag{8}$$

in which Γ_{max} and Γ_{min} are the value of Γ at the initial stage of loading and long term loading respectively. The parameter k_1 is a material parameter that determines the material viscoplastic degradation rate, Figure 2.

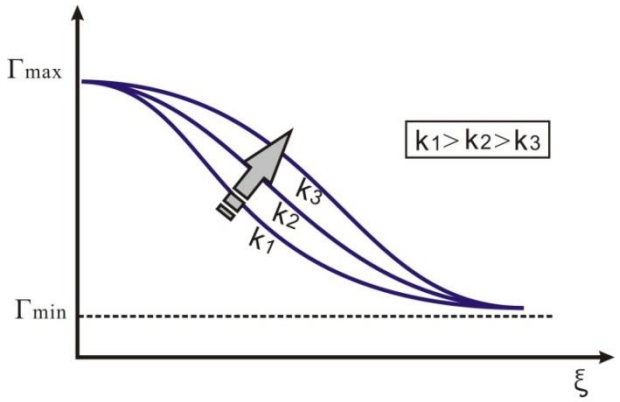

FIGURE 2 The influence of k_1 on Γ

In this thesis the equivalent viscoplastic strain ξ in Eq. (8) is termed as material "damage". It is computed from:

$$\xi = \int \left(\Delta \varepsilon_{ij}^{vp} \cdot \Delta \varepsilon_{ij}^{vp} \right)^{1/2} \tag{9}$$

where $\Delta \varepsilon_{ij}^{vp}$ is the incremental viscoplastic strain from Eq. (4).

The total stress at time $t + \Delta t$ can be computed by:

$$\boldsymbol{\sigma}_{t+\Delta t} = \boldsymbol{\sigma}^{e} - \mathbf{D}^{e} : \left(\Delta \varepsilon_{t+\Delta t}^{vp} + \Delta \varepsilon_{t+\Delta t}^{ve} \right) \tag{10}$$

where

$$\boldsymbol{\sigma}^{e} = \boldsymbol{\sigma}^{t} + \Delta \boldsymbol{\sigma}^{e} = \boldsymbol{\sigma}^{t} + \mathbf{D}^{e} : \Delta \varepsilon_{t+\Delta t} \tag{11}$$

is the "elastic predictor".

The incremental viscoelastic strain in Eq.(1) can be expressed as:

$$\Delta \boldsymbol{\varepsilon}_{t+\Delta t}^{ve} = \sum_{i=1}^{n} \left[{}^{i}\boldsymbol{\varepsilon}_{t}^{ve} \left(e^{-\Delta t/\tau_i} - 1 \right) + \Delta t \cdot e^{-\Delta t/2\tau_i} \mathbf{C}_{ve}^{i} \left(\frac{\sigma_{t+\Delta t} + \sigma_t}{2} \right) \right] \tag{12}$$

with $\mathbf{C}_{ve}^{i}$ being the compliance matrix of the viscoelastic component. The details of the derivation of Eq. (12) can be found in Collop et al. (*8*) and Scarpas (*6*).

On the basis of equations (4) and (12), the total stress at $t + \Delta t$ can be evaluated by means of Eq. (10) as

$$\begin{aligned} \boldsymbol{\sigma}_{t+\Delta t} = \boldsymbol{\sigma}^{e} &- \Gamma \cdot \langle \Phi \rangle \cdot \mathbf{D}^{e} : \frac{\partial Q / \partial \sigma}{\left\| \partial Q / \partial \sigma \right\|} \Delta t \\ &- \mathbf{D}^{e} \left\{ \sum_{i=1}^{n} \left[{}^{i}\boldsymbol{\varepsilon}_{t}^{ve} \left(e^{-\Delta t/\tau_i} - 1 \right) + \Delta t \cdot e^{-\Delta t/2\tau_i} \mathbf{C}_{ve}^{i} \left(\frac{\sigma_{t+\Delta t} + \sigma_t}{2} \right) \right] \right\} \end{aligned} \tag{13}$$

Flow Surface Characteristics

The flow surface which is used to describe the viscoplastic response of the material was proposed originally by Desai (*9*) and further developed by Liu (*10*).

The chosen form of the surface is given by:

$$F = \frac{J_2}{p_a^2} - \left[-\alpha \cdot \left(\frac{I_1 + R}{p_a} \right)^{n} + \gamma \cdot \left(\frac{I_1 + R}{p_a} \right)^{2} \right] = 0 \tag{14}$$

where I_1 and J_2 are the first and the second stress invariants, p_a is the atmospheric pressure with units of stress, R represents the triaxial strength in tension. In 3D space, Eq. (14) represents a

closed surface. The value of the yield function F determines the response of the material to a state of stress.

The value of α controls the size of the flow surface. It is typically defined as a function of deformation history. As α decreases, the size of the flow surface increases so this parameter controls the hardening of the material. When $\alpha = 0$, the ultimate stress response surface of the material is attained, Figure 3(a).

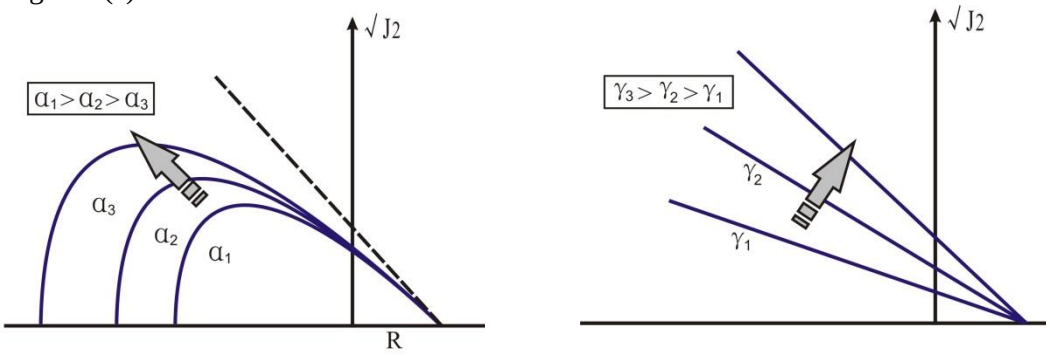

FIGURE 3 (a) Parameter α determines the size of the response surface. (b) Influence of γ on the ultimate strength surface

Parameter γ is related to the ultimate strength of the material. It denotes the slope of the ultimate strength response surface. As γ increases, the slope of the ultimate response surface increases, Figure 3(b).

The flow surface is fixed at its initial location during the loading cycles. The rate of the viscoplastic strain computed in Eq. (4) at time ‘‘t’’ is governed by the overstress i.e. the distance from the stress point to the yield surface, Figure 4. As a consequence, damage can accumulate as the number of stress excursions outside the viscoplastic response surface increases with the number of load cycles.

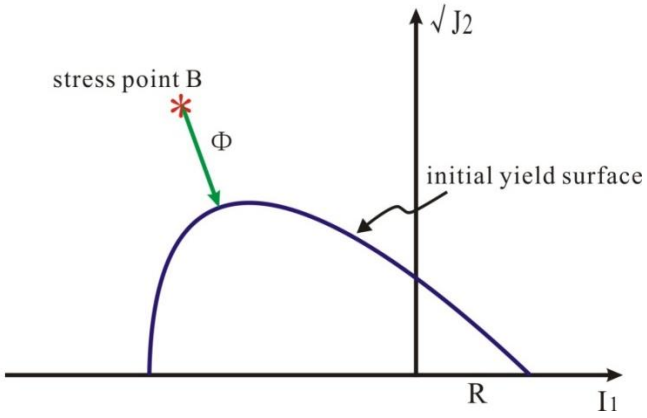

FIGURE 4 The concept of “overstress”

5PB FATIGUE TESTS ON MULTILAYER SURFACING BEAM SPECIMENS

This part is a further study of a research work presented on TRB 2012. More information about the 5PB tests is available (*7*). The mesh geometry of the 5PB test is shown in Figure 5. five membrane products (A1, A2, B, C1 and C2) ranked from MAT tests (*11*) were utilized as the top and bottom membrane layers in the 5PB beam tests. Four different beam surfacing structures have been tested and modeled, referred as surf. 1, 2, 3 and 4 by using the five membrane products, Figure 6.

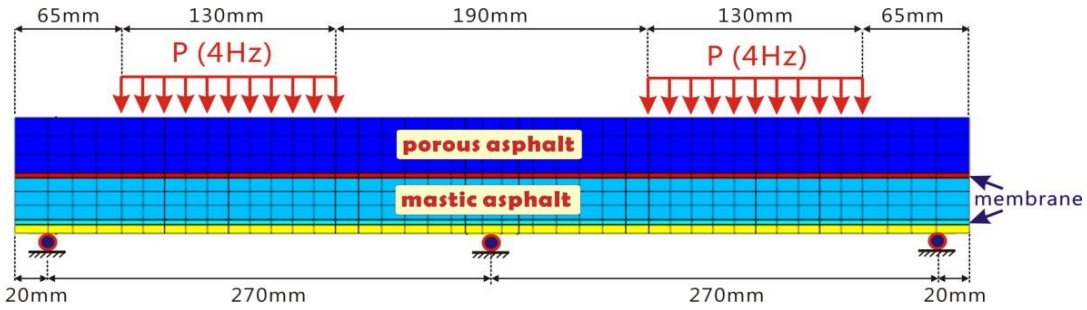

FIGURE 5 Geometry and boundary conditions of 5PB test FE model

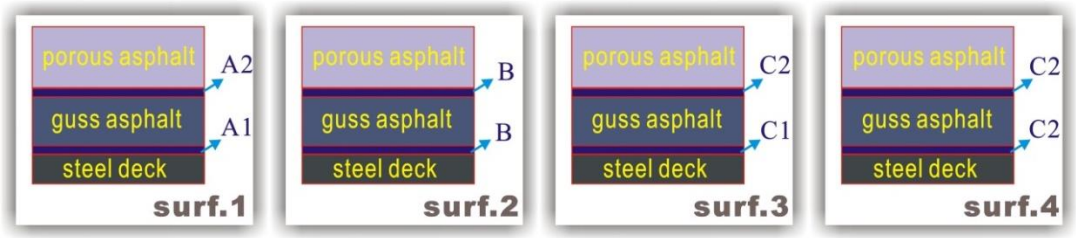

FIGURE 6 Four types of surfacing systems differing in membranes

MATERIAL PROPERTIES AND PARAMETERS

Relaxation tests according to EN 12311-1 were performed on these five membrane products for model parameter determination. Material parameters for PA and GA were decided based on the work done by Muraya (*12*) and Medani (*13*). The viscoelastic parameters for the five membrane products and the PA, GA layer are listed in Table 1. The steel deck layer is modeled as a linear elastic material. All parametric analyses were performed at 10 ^{o}C.

TABLE 1 Viscoelastic properties of surfacing materials

Property	A1	A2	B	C1	C2	PA	GA
E_1	6.19	5.7	4.59	9.24	9.38	200	450
Poisson's ratio	0.15	0.15	0.15	0.15	0.15	0.3	0.3
η	1876	1911	192	336.65	475.65	1	3
E∞	5.045	4.38	2.962	16.215	4.8	15750	15750

The methodology proposed by Scarpas et al. (*14*) and Liu (2003)(*10*) was adopted to determine damage model parameters for asphaltic materials. The material parameters of PA and GA layers, and the five involved membrane products are listed in Table 2.

TABLE 2 Initial yield surface parameters for modeling of surfacing materials

Parameter	A1	A2	B	C1	C2	PA(10^{o}C)	GA(10^{o}C)
Pa	-0.1	-0.1	-0.1	-0.1	-0.1	-0.1	-0.1
R	0.8	0.8	0.8	0.8	0.8	1.2	1.5
α	0.075	0.075	0.075	0.072	0.075	0.021	0.017
γ	0.108	0.108	0.105	0.11	0.11	0.072	0.072
n	2.15	2.15	2.15	2.15	2.15	2.4	2.4
g	2	2	2	2	2	2	2

In order to understand the physical phenomena of damage development inside the surfacing layers, the states of stresses under the load foot of 5PB test with respect to the initial yield surfaces of each individual layer material are plotted in Figure 7. The larger size of the yield surface indicates that the material behaves more elastically than the one with the smaller yield surface. The distance from

the stress point to the yield surface shows the potential of material generating damage during cyclic loading.

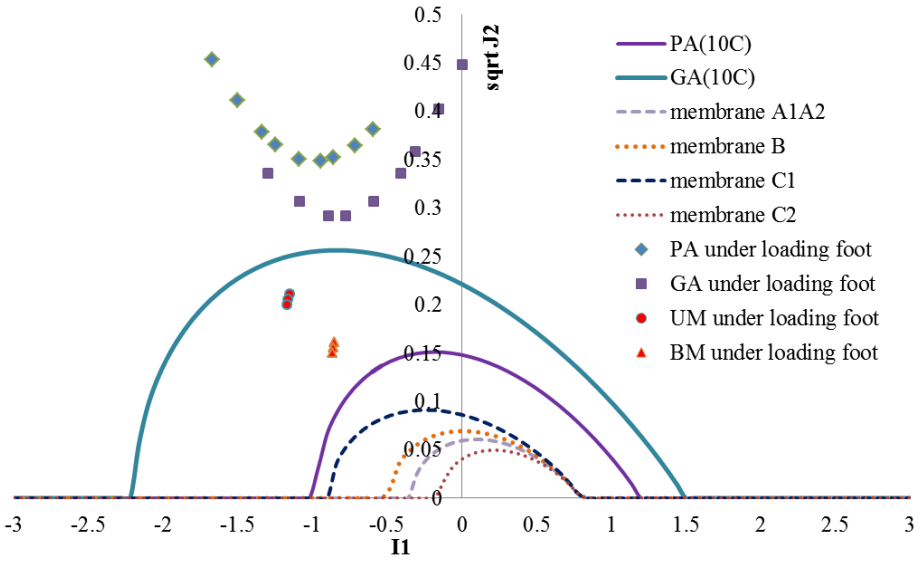

FIGURE 7 States of stresses and initial surfaces of surfacing materials

DAMAGE SIMULATIONS OF 5PB FATIGUE TESTS

In this section, the evolution of damage in different surfacing layers is investigated. The pressure load applied on each shoe was 0.707 MPa, corresponds with 9.2 kN on each shoe. Comprehensive laboratory 5PB fatigue tests of four multilayer surfacing structures were done in this research project (*11*). The simulations of 5PB tests with the four surfacing structures (Figure 6) are discussed in this section. Three main issues are investigated via the simulations of damage evolution of 5PB tests:

- Developments and distributions of damage in each individual surfacing material layer;
- Comparison of damage development in 5PB beams with four different surfacing structures;
- Investigation of the influences of the membrane bonding properties on damage evaluation.

Developments and Distributions of Damage in Material layers

Figure 8 shows a typical failure 5PB beam sample after a fatigue test in the lab. A 5PB beam subjected to 5000 cycles of sinusoidal beat load was simulated via CAPA-3D. The evolution of damages in the surfacing layers with increasing numbers of load cycles are presented in Figure 9.

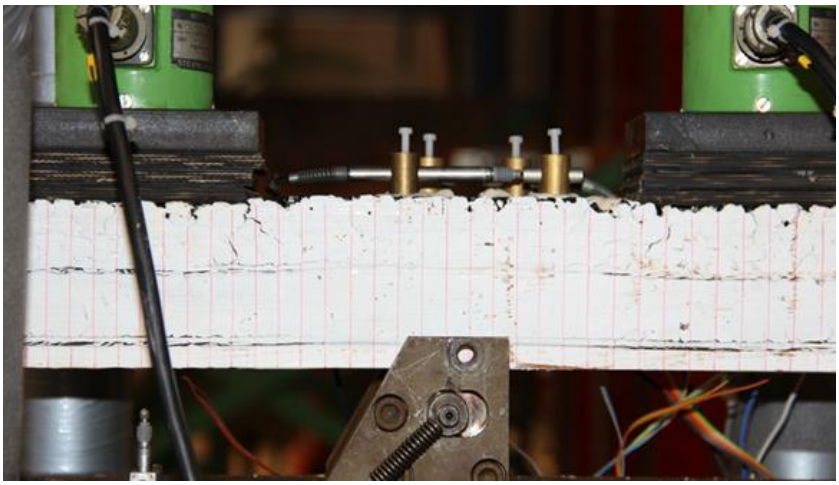

FIGURE 8 A 5PB failure sample

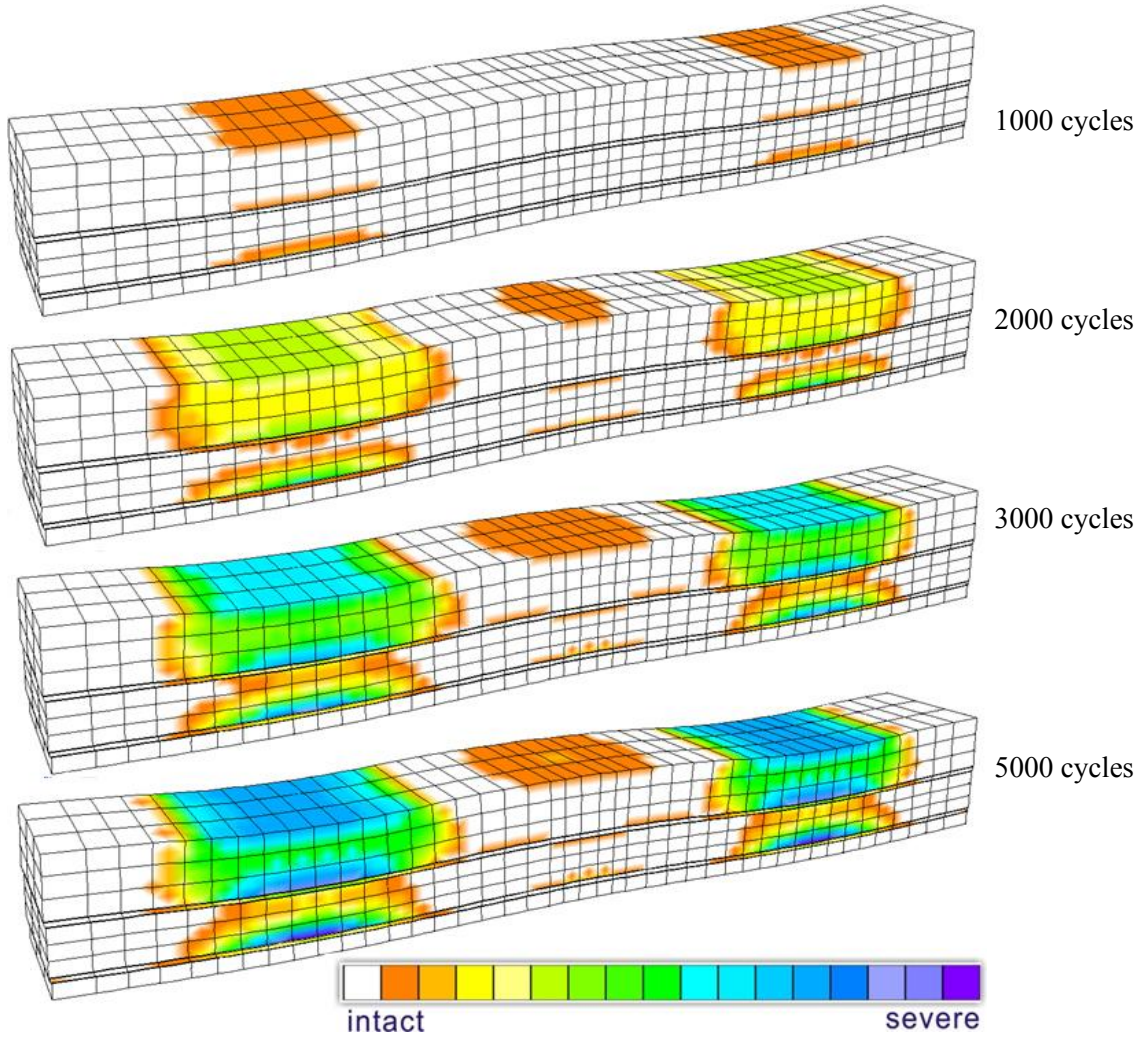

FIGURE 9 Evolution of damage in surfacing layers of 5PB test

The following observations are obtained from the results shown in Figure 8 & Figure 9:

- Damage is initiated firstly under the loading foots on the top of the PA layer, and the asphalt layers in the vicinity of the top of both membrane layers. It is then gradually propagated to the entire surfacing material layers. Damage appears on the top of the PA above the centre support soon afterwards.
- At the area under the loading foots, damage in PA layer developed both in the top-down and the bottom-top directions. While for GA layer, damage developed only from the bottom to the top.
- The damage area in the PA layer is wider than that of the GA layer. The larger damage is observed at the bottom of the GA and the PA layers, and on the top of the PA layer under the loading foots.
- Slight damage has occurred in the top surface of the specimen above the middle support. This phenomena is also observed by the lab specimen.
- More damage is accumulated in the vicinity of the top of the two membrane layers.
- By comparing the view of the 5PB failure sample in Figure 8, it shows that the proposed material model is capable of simulating correctly the damage or failure pattern in 5PB beam test.

Comparison of Damage in the Four Different Surfacing Structures

The maximum damage values of material layers for the four surfacing structures after a fatigue 5000 load cycles are illustrated in Figure 10.

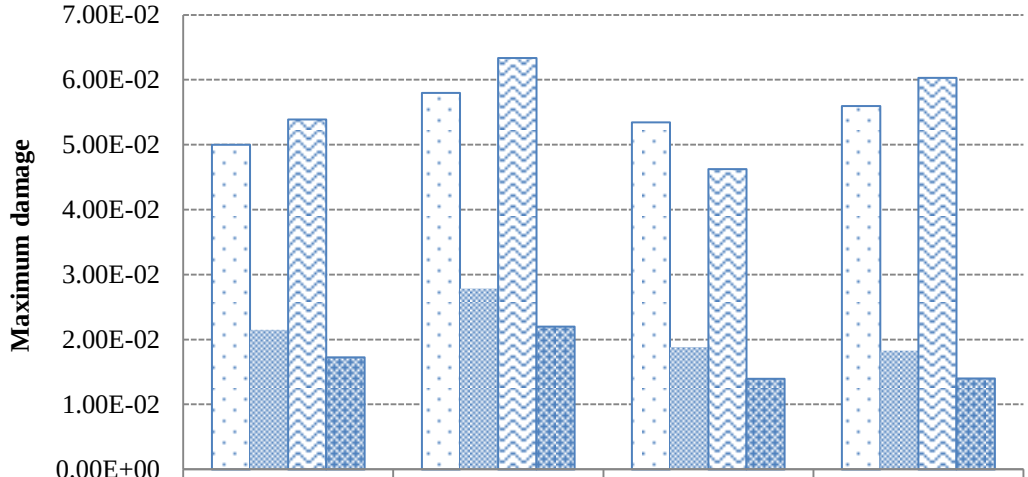

	surf.1	surf.2	surf.3	surf.4
Damage @ PA	5.00E-02	5.80E-02	5.35E-02	5.60E-02
Damage @ UM	2.15E-02	2.79E-02	1.89E-02	1.83E-02
Damage @ GA	5.39E-02	6.34E-02	4.63E-02	6.03E-02
Damage @ BM	1.73E-02	2.20E-02	1.40E-02	1.40E-02

FIGURE 10 Max. damage values in surfacing layers after 5000 load cycles

The following observations are obtained from the results shown in Figure 10.

- Overall, the least damage was observed in the surfacing system 3 (Figure 6), the severest damage occurred in surfacing structure 2. Damage in surfacing system 1 and 4 are comparable. This is highly in accordance with the observations from laboratory tests.
- The maximum damage on the GA layer is slightly higher than that of the PA layer in surfacing system 1, 2 and 4; However, for the surfacing system 3, damage on the PA layer is higher than the GA layer. This is due to a much stiffer bottom membrane layer in surfacing system 3 which provides a better composite action between the GA layer and the steel deck plate.
- Damage on top membrane layer is slightly higher than that of the bottom membrane layer.
- When we compare the simulation results together with material properties, a conclusion that stiffer membrane layers would reduce damage accumulated in the surfacing structure is approved. But, there is no clue about how the stiffness of membrane layers affects the service life of a surfacing structure.

Effect of Membrane Bonding Properties on Damages

It's known that composite actions between surfacing layers reduce stresses and stains in overlaying surfacing structure and result in a prolonged service life of the surfacing system. This desirable composite action demands for proper bonding between the various structural layers. A proper bonding interface between a membrane and its adhered material layer should with high resistance against shear deformation. Experience in the United States (Dublin Bridge in California), Switzerland (St. Albans Bridge in Basel), Germany (the Koln-Mulheim) tend to show that once the bond between the steel deck and surfacing is destroyed, the failure of the pavement is merely a matter of time.

By differing the shear stiffness of the four interface layers in a multilayer surfacing structure from 0.1 $N/mm^2/mm$ (stands for weak bonding condition) to 100 $N/mm^2/mm$ (represents a perfectly

bonded condition), simulations of fatigue tests of 5PBT were performed for surfacing structure 3 at 10 ^{o}C. Maximum damage values in surfacing layers were outputted and compared in Figure 11.

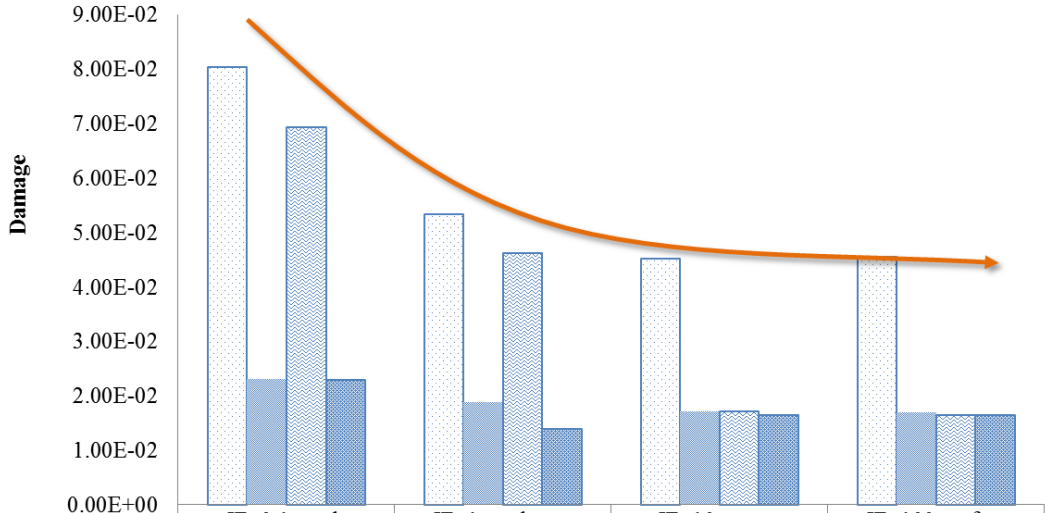

	IF=0.1 weak bonding	IF=1 moderate bonding	IF=10 strong bonding	IF=100 perfect bonding
Damage @ PA	8.05E-02	5.35E-02	4.53E-02	4.56E-02
Damage @ UM	2.31E-02	1.89E-02	1.73E-02	1.71E-02
Damage @ GA	6.94E-02	4.63E-02	1.73E-02	1.66E-02
Damage @ BM	2.30E-02	1.40E-02	1.66E-02	1.66E-02

FIGURE 11 Max. damage values in surfacing layers at various bonding conditions

The following important conclusions can be drawn.

- Better bonding conditions between surfacing material layers significantly reduce damage values in the surfacing structure;
- The reducing trend of damage occurred in surfacing layers with respect to enhancing bonding conditions is approximately an exponential decline line. After a state of fairly good bonding condition, damage values are not reduced anymore by improving the bonding condition;
- The damage values in PA and GA layers are reduced more significantly than those of both membrane layers.

CONCLUSIONS

- The numerical model is capable of simulating damage evolution in surfacing layers. It provides a proper tool for evaluating fatigue behavior of different surfacing systems.
- The five-point bending test offers a good tool in studying the composite behaviour of the multilayer surfacing system on OSDBs;
- Stiffer membranes used in surfacing structures could reduce damages in surfacing materials;
- Better bonding properties of membranes significantly postpone the occurrence of damages and reduce the accumulated damage values. However, after a certain point, enhancing the bonding properties of membranes won't reduce the damages anymore.

ACKNOWLEDGMENT

This work is part of the research program of InfraQuest. InfraQuest is a collaboration between Rijkswaterstaat, TNO and the Delft University of Technology. This research project is partially funded by the Dutch Transport Research Centre (DVS) of the Ministry of Transport, Public Works and Water Management (RWS). Their financial support is highly appreciated.

REFERENCES

1. Gurney, T. *Fatigue of steel bridge decks*. HMSO Publication Centre: London, 1992, pp. 165.
2. Wang, C. S., Feng, Y. C., & L. Duan. Fatigue Damage Evaluation and Retrofit of Steel Orthotropic Bridge Decks. *Key Engineering Materials*, 413, 2009, pp. 741-748.
3. Miner, M. A. Cumulative Damage In Fatigue. *Applied Mechanics*, Vol. 12(9), 1945.
4. Kim, Y. R. and D. N. Little. One-dimensional Constitutive Modelling of Asphalt Concrete. *Journal of Engineering Mechanics*, 116(4), 1990, pp. 751-772.
5. Lee, H. J. and Y. R. Kim. Viscoelastic constitutive model for asphalt concrete under cyclic loading. *Journal of Engineering Mechanics*, 124(1), 1998, pp. 32-40.
6. Scarpas, A. *A mechanics based computational platform for pavement engineering*. PhD thesis, Delft University of Technology, 2004.
7. Li, J., Liu, X., Scarpas, A. et al. Analysis of five-point bending test for multilayer surfacing systems on orthotropic steel bridge. In proceeding of *Transportation Research Record: Journal of the Transportation Research Board,* Washington D.C., 2013.
8. Collop, A. C., Scarpas, A., Kasbergen, C., & A., de Bondt. Development and finite element implementation of stress-dependent elastoviscoplastic constitutive model with damage for asphalt. In *Transportation Research Record: Journal of the Transportation Research Board*, No. *1832*(1), Transportation Research Board of the National Academies, Washington, D.C., 2003, pp. 96-104.
9. Desai, C. S. A general basis for yield, failure and potential functions in plasticity. *International Journal for Numerical and Analytical Methods in Geomechanics*, 4(4), 1980, pp. 361-375.
10. Liu, X. *Numerical modelling of porous media response under static and dynamic load conditions*. PhD thesis, Delft University of Technology, 2003.
11. Liu, X., & A. Scarpas. *Experimental and Numerical Characterization of Membrane Adhesive Bonding Strength on Orthotropic Steel Deck Bridges*. Project report. Delft University of Technology, 2012
12. Muraya, P. M. *Permanent deformation of asphalt mixes*. PhD thesis, Delft University of Technology, 2007.
13. Medani, T. O. *Design principles of surfacings on orthotropic steel bridge decks*. PhD thesis, Delft University of Technology, 2006.
14. Scarpas, A., Al-Khoury, R., Van Gurp, C. A. P. M., & S. M. J. G. Erkens. Finite element simulation of damage development in asphalt concrete pavements. In *Eighth International Conference on Asphalt Pavements* (No. Volume I), 1997.